SCATHA Retrospective: Satellite Frame Charging and Discharging in the Near-Geosynchronous Environment

M.S. Gussenhoven[1] and E.G. Mullen[2]

[1]Air Force Research Laboratory, Space Vehicles Directorate, Hanscom AFB, MA 01731

[2]Assurance Technology Corporation, Carlisle, MA 01741

Abstract

The major results obtained from the SCATHA satellite on frame charging are: a) Verification of satellite to plasma potential measurements in sunlight by means of an electric field experiment on a 50m boom; b) Identification of the electron environment that drives charging; c) Clarification of the magnetospheric dynamics that produce the charging environment; d) Determination of the difference between sunlight and eclipse charging and its implications for achieving current balance to the spacecraft; e) Demonstration that emitted electron beams can charge and discharge the host satellite, but may return, highly focused, to the vehicle.

I. INTRODUCTION

The Air Force SCATHA (Spacecraft Charging AT High Altitude) Program was developed at a time when spacecraft charging was clearly recognized as a possible hazard, but instances of charging were poorly reported and recorded. The SCATHA satellite was launched in January, 1979, a scant 7 years after publication of the seminal spacecraft frame charging paper by DeForest [1]. The SCATHA satellite was instrumented specifically to study the occurrence of charging, the environment which leads to charging, and potential means of mitigating charging [2]. Two types of charging were studied: frame charging and deep dielectric charging. Two types of discharging were also studied: spontaneous discharging, by breakdown somewhere on the satellite, and controlled discharging by emitters. This retrospective covers frame charging and controlled discharging by emitters.

Spacecraft frame charging occurs because without it there would be current imbalance to the spacecraft: the spacecraft to plasma potential difference adjusts currents to achieve current balance to the spacecraft. In the geosynchronous environment, in sunlight, the current balance equation is:

$$- I_e + I_i + I_{se} + I_{be} + I_{pe} = 0 \qquad (1)$$

Here I_e and I_i are the currents attributable to the total electron and ion ambient populations, and I_{se}, $I_{be,}$ and I_{pe} are the secondary electrons, backscattered electrons and photo-electrons, respectively, which emanate from the satellite. The photoelectron number flux for typical satellite materials is on the order of 10^{10} $(cm^2s)^{-1}$. The ambient electron number flux can, at times, reach several times 10^{10} $(cm^2s)^{-1}$, and the ambient ion flux is about 1-2 orders of magnitude lower than either of the electron number fluxes: 10^8 - 10^9 $(cm^2s)^{-1}$. The secondary and backscattered electron populations depend on spacecraft materials and on the incoming electron spectrum, but the total can be shown to be a fair fraction, if not more than, the incoming electron population [3, 4]. Thus, it is difficult to see how the combination of the first four terms in Eq. 1 can balance the photoemission, or, in other words, how sunlight frame charging can occur at all.

In the late 1970's the worst cases of satellite frame charging were known to occur in the geosynchronous region during satellite eclipse, that is, in the absence of I_{pe}. In this case the net electron current, $- I_e + I_{be} + I_{se}$, decelerated by the potential difference between the spacecraft and plasma, is balanced by the ambient ion current, accelerated to the spacecraft by the potential difference. The acceleration of ions can be seen in particle detectors as a peak in that energy channel which represents the frame to plasma potential difference. Until the SCATHA satellite was flown this was the common method of detecting satellite frame charging.

At the time of the SCATHA launch, there were many efforts to model the spacecraft charging process, both analytical (with simple space systems and one- or two Maxwellian particle distributions) and computer-generated (with complex material configurations representing the satellite and actual particle distributions). Our approach to analyzing the SCATHA satellite data was to see what conclusions about the charging process could be derived from the data alone, independent of the modeling process. Five major results were forthcoming and are reviewed, in turn, in the following Sections. The initial reporting of these results can be found in three papers which also give details on the satellite instrumentation [5, 6, 7]. The processed particle and field data are published in two volumes [8].

II. HIGH TIME RESOLUTION MEASUREMENTS OF SPACECRAFT POTENTIAL

The electric field detector on SCATHA consisted of two 50m antennas that form a 100m dipole. The inner 30m of each antenna was coated with Kapton insulation so that the outer 20m conduction surfaces of copper beryllium acted as a double floating probe ensemble to measure dc electric fields in the ambient plasma. The instrument also measured the voltage difference between one of the antennas and spacecraft ground. When the conducting tip floats at plasma potential, this mode of operation provides high-time resolution (twice per second) measurement of the satellite frame potential with respect to the ambient plasma potential, ϕ_f. The materials and length of the booms should guarantee this to be the case in sunlight for satellite potentials less than ~1kV to within an accuracy of several volts.

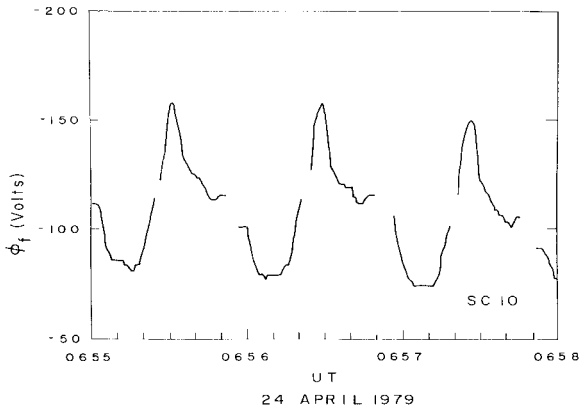

Figure 1. Frame potential for three satellite spins on 24 April 1979

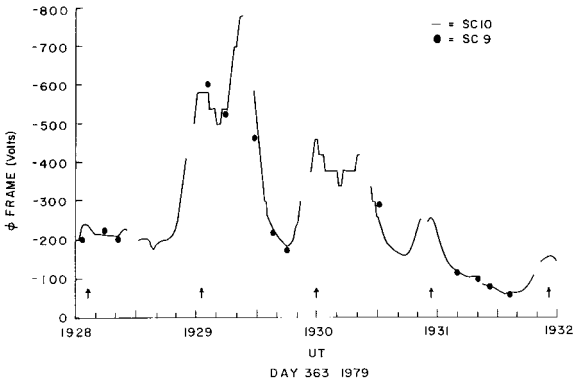

Figure 2. Comparison of two methods of measuring frame potential for the three highest charging events

The three cases of largest sunlight charging during the first year of SCATHA operations were on 24 April, 29 August and 29 December, all in 1979. The charging was determined by ion peaks in the particle detector and measured by the electric field experiment. Figure 1 shows the electric field measurements during the 24 April event for three spin periods of the satellite A strong modulation of the potential with satellite orientation is evident. Data gaps occur twice per spin when the electric field booms were shadowed and did not give accurate readings. The value of ϕ_f as determined from the electric field experiment agrees with that from the ion peak measurement only if the exact time in the satellite spin is used to compare the two measurements, as shown in Figure 2 (the charging event on 29 December 1979), where the individual points are from the ion peak method. The statistical agreement between the two methods for the three highest charging events is shown in Figure 3, again using only points (250 points total) taken at exactly the same time. The regression coefficient for a straight line fit between the two methods is 0.99.

Figure 2 points up a potential problem with the ion peak method for determining potentials on spinning satellites. Unless the ion peaks are measured at the same point in every spin, ambiguous results will occur when attempting to match charging levels with other phenomena. Another consequence of the excellent agreement between the two methods is confirmation that the sheath size around the satellite in sunlight is well within 30m for ϕ_f up to -800 volts. Using the same point in each spin, a data base of the SCATHA frame potential was created for event and statistical studies. The spin position chosen was that for which ϕ_f had the largest absolute value during relatively stable charging periods, such as shown in Figure 1. A daily charging profile, created in this way, is shown in Figure 4 for 24 April 1979, the smallest of the three highest charging events.

III. What Drives Spacecraft Frame Charging

Figure 4 shows a sharp onset of the frame potential (here positive values indicate a negatively charged frame) at 06:45 UT (23.1 MLT) when SCATHA was just entering the plasma sheet. The peak potential was -320 V. The potential was variable, and remained high until onset of eclipse at 07:13 UT. Figure 5 shows the relationship between frame potential in sunlight and the omnidirectional number flux in 3 ambient populations: a) 50 eV-400 keV ions (triangles), having the lowest intensity; b) 50 eV-30 keV electrons (crosses), having the highest intensity; and c) 30-400 keV electrons (circles), having intermediate intensities. The frame potential shows no systematic relationship to either the ions or the low energy electrons, but is directly proportional to the high energy electron number flux. The lack of correlation of frame charging with the low energy population and the excellent correlation with the high energy electron population was found

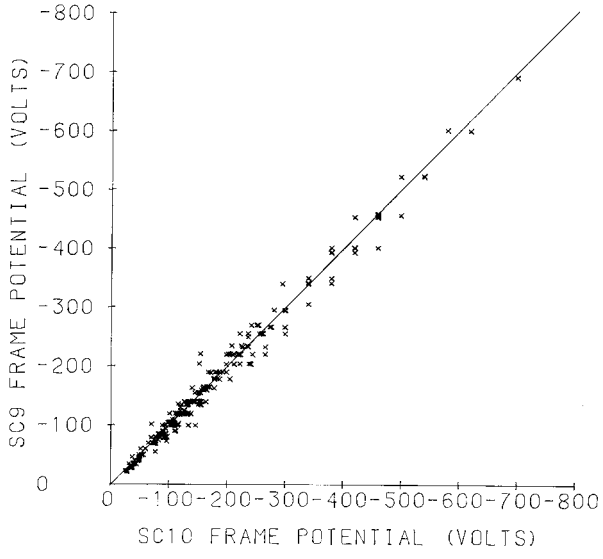

Figure 3. Comparison of frame potential as measured by the electric field experiment (continuous line) and the ion peak method (dots) on 29 December 1979

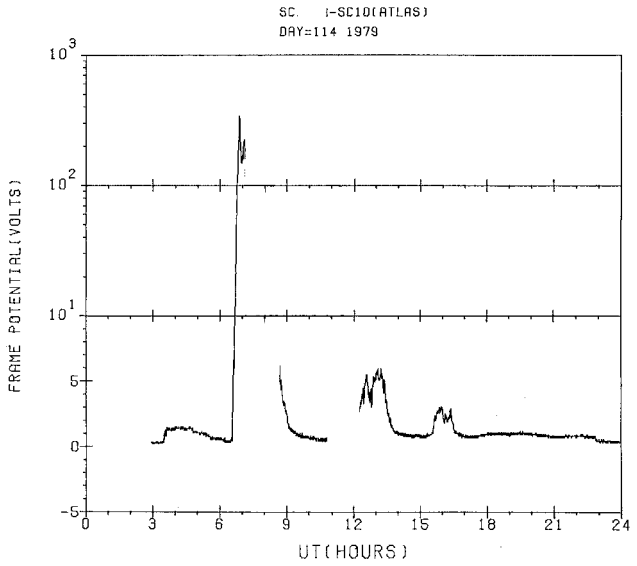

Figure 4. Frame potential in sunlight on 24 April 1979 using the electric field experiment

in all the other high level sunlight charging cases studies. In fact, when frame charging was found in the low altitude DMSP satellites, in darkness, the charging magnitude was driven by the >10 keV electron number flux, and was uncorrelated with the larger, lower energy number flux [9]

There are several immediate consequences of finding that the high energy electron population drives spacecraft frame charging. The first is that the low energy population must be essentially self-balanced by its own backscatter and secondary populations. This has been turned into the notion of a critical temperature, below which a Maxwellian electron population is self-balanced by its own backscattered and secondary populations, and thus, has little effect on charging the spacecraft [3,4]. It is also the case that secondary and

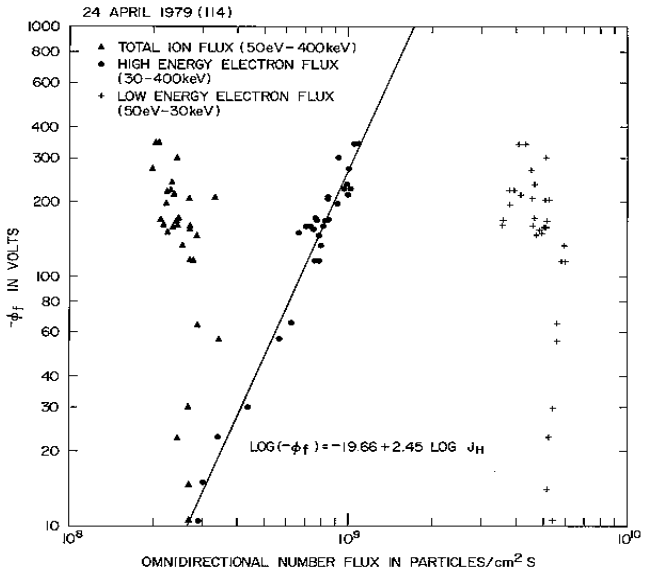

Figure 5. Frame potential on 24 April 1979 as a function of ion, high energy electron, and low energy electron number flux

backscattered populations fall off with energy [10], rendering the high energy population more effective in charging the vehicle. If we represent the current of the ambient electron population by two contributions: I_{eL} and I_{eH}, the low and high energy populations, respectively, then:

$$-I_{eL} + I_{be} + I_{se} = 0 \quad (2)$$

is the self-balancing condition, and

$$-I_{eH} + I_i + I_{pe} = 0 \quad (3)$$

is the new condition for current balance. Since the ion current is much smaller than the two electron currents, we conclude that it is primarily photoemission that balances the charging current. Much of the photoemission must return to the vehicle when it is charged, since it is potentially so much larger than the high energy electron flux.

Another consequence of the identification of the >30 keV electron population as the driver of spacecraft charging in sunlight, is that the occurrence of charging will be found statistically where the occurrence of the high energy population occurs, and charging will be directly related to processes that produce the high energy electron population. When statistical studies were performed on the occurrence of sunlight frame charging on SCATHA little variation was found with altitude (5.5-8.5 R_E) or magnetic latitude ($\pm 18^o$). However, there was a significant dependence on local time and on magnetic activity, as measured by Kp. Figure 6 shows the dependence of the occurrence of sunlight charging as a function of local time. Figure 7 shows the average number flux of four ambient particle populations as a function of local time L-shell and Kp. The local time region having no frame charging > 10V is on the dayside from 9 - 19 MLT. This is where the high energy electron flux falls below about 2 x 10^8 $(cm^2 s)^{-1}$. Note that there is little dependence of the high energy electron population on altitude (over the altitude range of SCATHA), but a strong dependence on Kp. The occurrence of charging increases with Kp up to Kp=5, after which it tends to level off. This is similar to the Kp profile of the high energy number flux in Figure 7.

IV. Eclipse Charging

Figure 8 shows the frame potential in eclipse determined by the ion peak method (solid line). Before entering eclipse the frame charging was near -100 V. This jumped to -6000 V in eclipse. One order of magnitude is usually given as the rule of thumb conversion between the two, in the same environment. It is somewhat higher in this case. In eclipse the frame potential remained reasonably constant between 4 and 8 kV for about 1/2 hr, after which it decayed to lower values.

If the low energy electron population remains self-balancing during the high eclipse charging (as is the case for a self-balancing Maxwellian distribution), then, in the absence of photoemission the equation for current balance to the spacecraft is

$$-I^*_{eH} + I^*_i = 0 \quad (4)$$

The electron and ion currents are starred because a frame potential between -4 and -8 kV will severely alter the incident

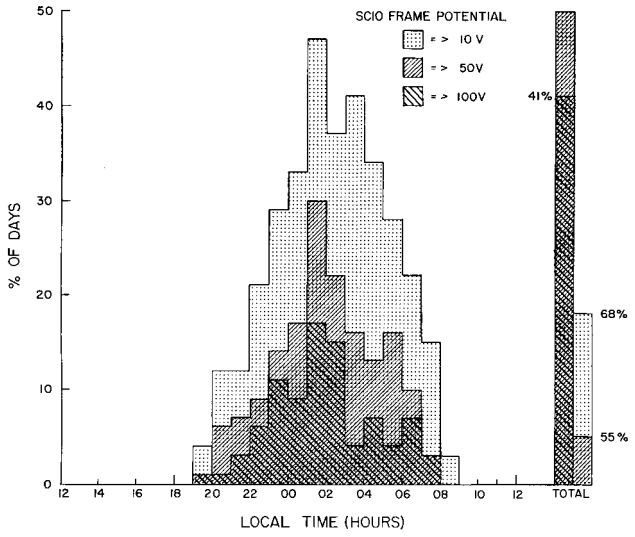

Figure 6. Percentage occurrence of three levels of frame potential as a function of magnetic local time

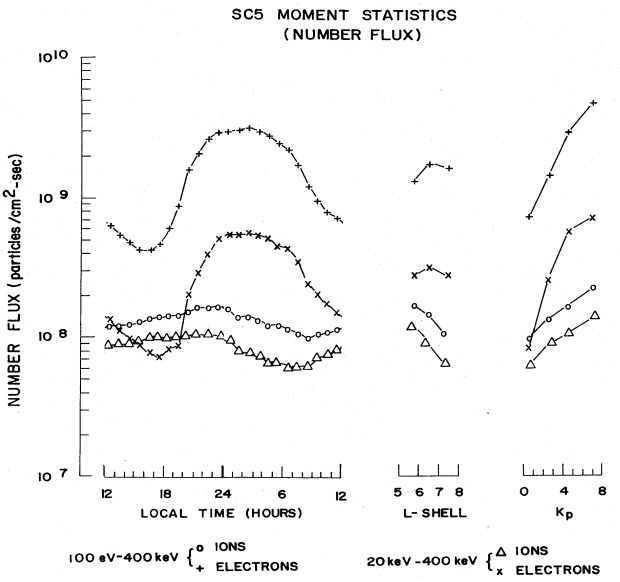

Figure 7. Average total and high energy number flux of electrons and ions as a function of magnetic local time, altitude and magnetic activity

currents (retard electrons and accelerate ions). For April 24 1979, the high energy electrons had temperatures of ~13 keV. Thus the current from these electrons could be halved by the large eclipse potential. In eclipse, the potential continued to be highly correlated with the 30-100 keV electron fluxes, as measured on the vehicle, even though these fluxes showed fractional decreases with eclipse onset. The cold ions were virtually absent before and during the charging period, although in eclipse, ions in the 4-20 keV range increased by factors up to an order of magnitude along the magnetic field lines, and by lesser amounts perpendicular to the field.

V. Creating the High Energy Electron Environment

We next look, in more detail, at the charging event on 24 April 1979, during sunlight. Figure 9 shows the measured and model magnetic field magnitude (top panel), the total number flux for electrons >50 eV (second panel), the high energy (>30 keV) electron number flux, (third panel) and the negative of the frame potential (bottom panel). Again we see that the total electron population bears little relationship to the frame potential, while the high energy electron population and the frame potential variations track each other. Also clear is the similarity between the magnetic field variation and that of both frame potential and high energy electrons.

Figure 10 is a plot of the natural logarithm of the electron and ion distribution functions as a function of magnetic moment (energy/magnetic field magnitude) for points perpendicular to the magnetic field (pitch angle 90°) and for the period over which the sharp increase in B, high energy number flux and frame potential occur (6:40-6:50 UT). Quite clearly the points for each species all fall on the same line. This suggests that the particles have been adiabatically accelerated by the increasing magnetic field. Such interpretation of the data is supported by the fact that the electron and high energy ion distribution functions parallel to the magnetic field did not change throughout this period. In each of the three cases of highest charging, an increased high energy electron population was associated with a sharp increase in the magnetic field (snap of the field back to a quiet model value).

The April 24 charging event occurred during a period of Kp = 3+. The other two highest charging events occurred during periods when Kp was 7- and 5 (in order of occurrence). In these latter two cases the sharp increase in the magnetic field was part of a dipolarization process following magnetotail stretching, the whole process taking several hours. We can associate both periods with intense, and, in one case, multiple substorm activity. But the April 24 event was not like that. The magnetic indices, Kp, Dst and AE are shown in Figure 11 for 21-24 April, 1979. There had been a period of moderately high Kp on 22 April (6-) which slowly decayed

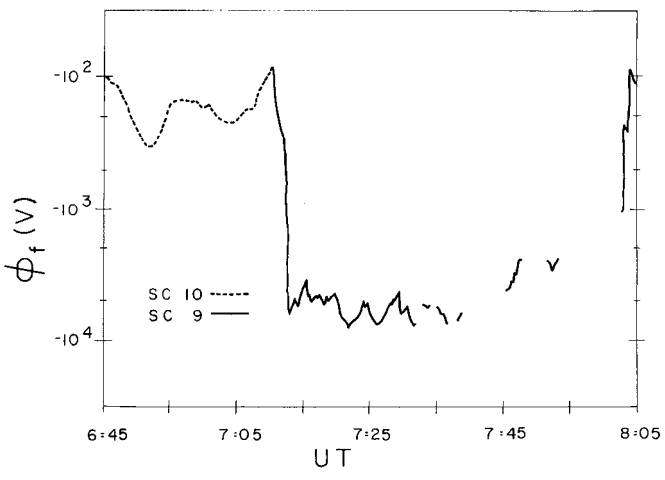

Figure 8. Frame charging in sunlight (dashed line) and in eclipse (solid line) on 24 April 1979

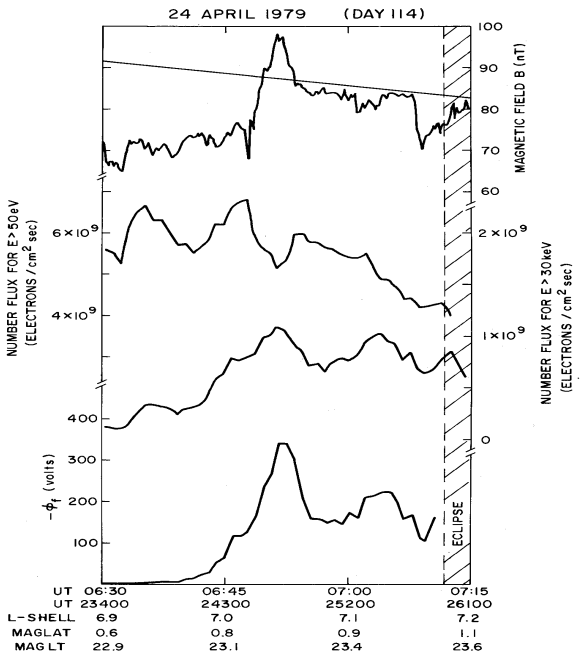

Figure 9. Detailed look at electron flux, magnetic field magnitude and frame potential as a function of time, during the high sunlight charging period on 24 April 1979

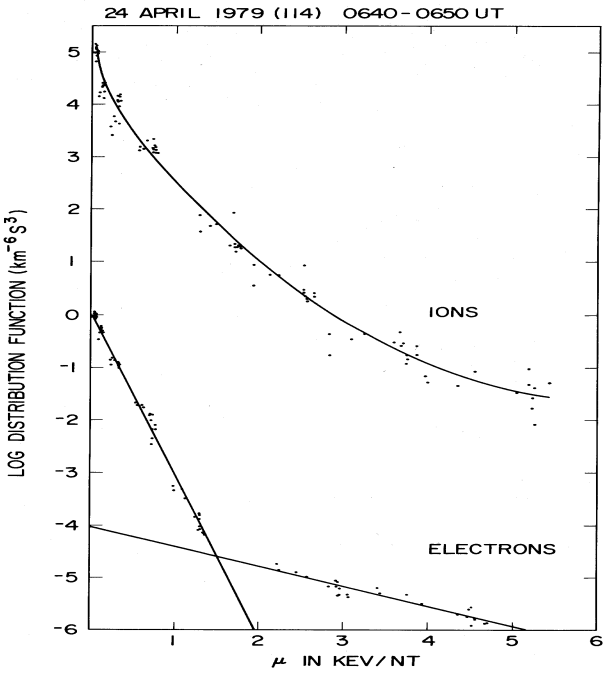

Figure 10. Ion and electron distribution function taken perpendicular to the local magnetic field as a function of magnetic moment during the high sunlight charging period on 24 April 1979

through 24 April. The period around 07 UT, when the high level charging occurred, is quite ordinary. Also there is no clear indication in the solar wind data of the cause of the current disruption that allowed the magnetic field to return to the quiet model value. High charging events, like this one, may be extremely difficult to anticipate. The April 24 event has been reported in great detail [11].

VI. Electron Beam Operations

Several techniques to actively charge and discharge the satellite were used on SCATHA [12]. One was by means of an electron beam system that emitted only electrons over a wide range of energies and currents. At the highest current and beam energy levels (used only on 30 March 1979) beam operations led to severe arcing problems on the spacecraft and the loss of a scientific instrument [13]. They were discontinued thereafter. The effects of operating the electron beam are summarized as follows [14]: a) It is possible to positively charge a vehicle or discharge a negatively charged vehicle using an electron beam emitter on a spacecraft. b) Above a beam voltage threshold, which depends on conditions in the ambient environment, the charging level is a function of beam current only as long as the ambient environment has sufficient electrons to provide charge balance and until the potential difference between the ambient plasma and the satellite reaches beam energy. c) The charging level depends on the ambient plasma. Higher charging levels are found in the hot, low density plasma sheet, than in the dense, cold plasmasphere. d) At currents much higher than necessary for the ambient plasma-frame potential difference to reach beam energy, the vehicle potential drops slightly and a portion of the beam returns to the spacecraft to provide current balance. The beam return can be highly localized and focused.

The last effect is shown in Figure 12. Beam return to the satellite could be seen the particle detector that always pointed near perpendicular to the local magnetic field. Figure 12 shows the data from this detector when a three keV beam was emitted at 0.1 mA in the plasma sheet, in both sunlight and eclipse conditions, on 30 Mar 1979. These conditions caused the satellite to charge positively to ~2.9 kV. From previous

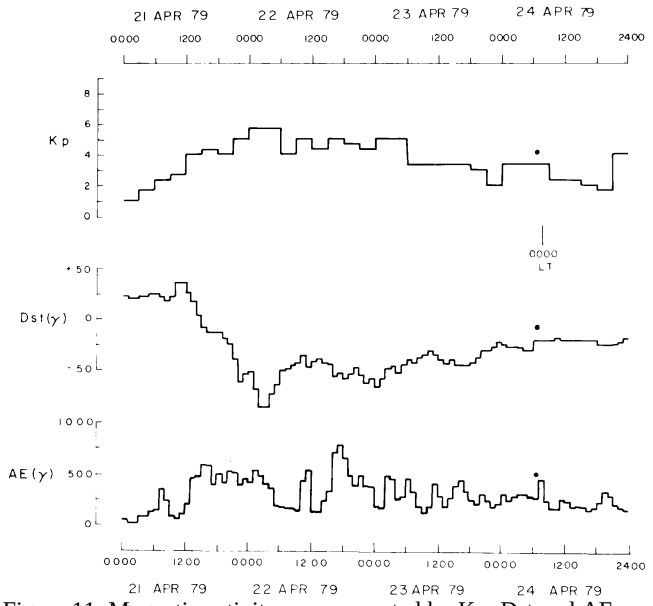

Figure 11. Magnetic activity as represented by Kp, Dst and AE as a function of time from 21-24 April 1979

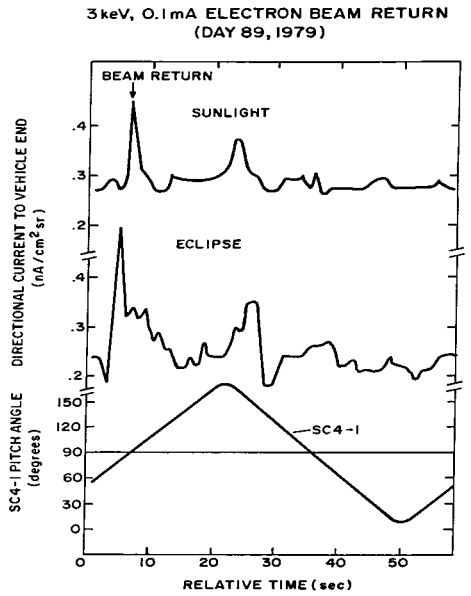

Figure 12. Return current to the vehicle in the 3 keV energy channel in sunlight and eclipse, and orientation of the emitted beam as a function of time.

beam operations it was found that the midnight plasma sheet region can supply something less than 0.1 mA, so it is not surprising that the electron beam must return to the vehicle to achieve current balance. The detectors perpendicular to the magnetic field will only be in a position to see the returning beam when the beam itself is emitted near-perpendicular to the magnetic field. This is shown to be the case both in sunlight and eclipse in Figure 12 where the measured current (top two panels) and the beam pitch angle (bottom panel) are shown. The beam is quite sharply focused. The return of the beam in this plane, can be shown to be achieved for quite simple but reasonable electric and magnetic configurations around the spacecraft [15].

VII. Conclusions

The SCATHA program advanced our understanding of how satellites charge and discharge. It quantified many aspects of frame charging in sunlight and eclipse. Most of these results are now incorporated into spacecraft charging codes, into magnetospheric programs to forecast charging environments and in instruments designed to detect and mitigate high levels of surface charging.

References

[1] S.E. DeForest, "Spacecraft charging at synchronous orbit," *J. Geophys. Res., 77*, 651, 1972.

[2] J.R. Stevens and A.L. Vampola, eds., *Description of the Space test Program P78-2 Spacecraft and Payload, Rep. SAMSO TR-78-24*, Air Force Syst. Command, Los Angeles, CA, 1978.

[3] J.G. Laframboise, R. Godard, and M.. Kamitsuma, "Multiple floating potential, 'threshold temperature' effects and 'barrier' effects in high voltage charging of exposed surfaces on spacecraft," *Eur.Space Agency Spec.* Pub., *ESA SP-178*, 269, 1983.

[4] S.T. Lai, M.S. Gussenhoven, and H.A. Cohen, "The concepts of critical temperature and energy cutoff of ambient electrons in high voltage charging of spacecraft," *Eur.Space Agency Spec. Pub., ESA SP-178*, 169, 1983.

[5] E.G. Mullen and M.S. Gussenhoven, *SCATHA Environmental Atlas, Tech. Rep. AFGL-TR-0002, ADA131456*, Air Force Geophysics Laboratory, Hanscom AFB, MA, 1983.

[6] E.G. Mullen, *et al.*, "SCATHA survey of high-level spacecraft charging in sunlight," *J. Geophys. Res., 91*, 1474, 1986.

[7] M.S. Gussenhoven, E.G. Mullen and D.A. Hardy, "Artificial charging of spacecraft due to electron beam emission," *IEEE Trans. Nucl. Sci., NS-34*, 1614, 1987.

[8] E.G. Mullen and M.S. Gussenhoven, *SCATHA Atlas Data Base, Volumes I and II, GL-TR-89-0249(I, II)*, Air Force Geophysics Laboratory, Hanscom AFB, MA, 1989.

[9] M.S. Gussenhoven, *et al.*, "High-level spacecraft charging in the low-altitude polar auroral environment, *J. Geophys. Res., 90*. 11009, 1985.

[10] Ira Katz, Myron Mandell, Gary Jongeward and M.S. Gussenhoven, "The importance of accurate secondary electron yields in modeling spacecraft charging," *J. Geophys. Res., 91*, 13739, 1986.

[11] E.G. Mullen, M.S. Gussenhoven and H.B. Garrett, *A 'Worst Case' Spacecraft Environment as Observed by SCATHA on 24 April 1979, AFGL-TR-81-0231*, Air Force Geophysics Laboratory, Hanscom AFB, MA, 1981.

[12] H.A. Cohen, *et al.*, " A comparison of three techniques for discharging satellites," in *Proceedings, Spacecraft Charging Conference*, N.J. Stevens, and C.P. Pike, eds., *AFGL-TR-81-0270*, Air Force Geophysics Laboratory, Hanscom AFB, MA, 1981.

[13] H.A. Cohen et al., *et al*. "P78-2 satellite and payload responses to electron beam operations on March 30, 1979," in *Proceedings, Spacecraft Charging Conference*, N.J. Stevens, and C.P. Pike, eds., *AFGL-TR-81-0270*, Air Force Geophysics Laboratory, Hanscom AFB, MA, 1981.

[14] M.S. Gussenhoven, E.G. Mullen and D.A. Hardy, "Artificial charging of spacecraft due to electron beam emission," *IEEE Trans. Nucl. Sci., NS-34*, 1614, 1987.

[15] M.S. Gussenhoven, *et al*., "Analysis of ambient and beam particle characteristics during the ejection of an electron beam from a satellite in near-geosynchronous orbit on March 30, 1979," in *Proceedings, Spacecraft Charging Conference*, N.J. Stevens, and C.P. Pike, eds., *AFGL-TR-81-0270*, Air Force Geophysics Laboratory, Hanscom AFB, MA, 1981.